Short-range interactions in the effective theory for Wilson lines

Joe Kiskis
Department of Physics, University of California, Davis, California 95616
(Received 30 September 1987)

The effective theory for Wilson lines results from integrating over the variables of the finite-temperature gauge theory while holding the values of the lines fixed. A quantity which measures the range of interaction in the effective theory is introduced. It is approximated in a Monte Carlo simulation at two points near the confinement-deconfinement phase transition. The results show an interaction range of less than one lattice unit.

I. INTRODUCTION

The order parameter of the confinement-deconfinement phase transition in pure gauge theory is the Wilson line. An effective theory for the lines can be obtained by integrating out all other degrees of freedom in a finite-temperature gauge theory. The line theory inherits a global-symmetry group that is the center of the gauge group of the parent theory. The phase transition is associated with spontaneous breakdown of this global symmetry.[1]

If the effective theory has short-range interactions and the phase transition is second order, then it should lie in the universality class that contains models of the same symmetry and spatial dimension. If so, the critical exponents for the confinement-deconfinement phase transition will coincide with those of the other members of the class.

SU(2) gauge theory at finite temperature in three spatial dimensions is the subject of this paper. The effective theory for the lines is three dimensional and has a global $Z(2)$ symmetry. The three-dimensional Ising model is a simple representative of the same universality class. All indications[2,3] are that the gauge theory's phase transition is second order. The critical exponents that have been measured are consistent with those of the Ising model.

This paper addresses the range of interaction in the effective theory. There are theoretical arguments[1] for short-range interactions at both strong and weak coupling. However, it is the intermediate region around the critical point that is important. Lattice regularization and numerical methods can be used to measure the range of interaction near the phase transition. An operator which yields this information is introduced in Sec. II. It is cast into a form that can be used in a Monte Carlo simulation. The numerical methods and results are present in Sec. III. The simulation was done at two points close to the critical point in the confined phase. The result is a range of interaction around 0.5 lattice units. Earlier work[3] measured line-line correlation lengths of 4.5 and 6.25 lattice units at these points. Section IV contains a brief conclusion.

The method provides a direct determination of a general property (the interaction range) of the effective theory. The operator that is used gives a measure of the interaction range that is independent of the form of the effective theory. It is not necessary to postulate a specific expression for the effective theory.

This work is the first step in a larger effort to study the structure of the effective theory as a function of the gauge theory parameters N_T and g^2. The goal is to identify those changes in the effective theory that drive the phase transition and to understand their origin in the underlying gauge theory.

Related work on other models can be found in Ref. 4.

II. THEORY

This section discusses the effective theory for the Wilson lines and its relation to the underlying gauge theory. This relationship can be used to find correlation functions in the finite-temperature gauge theory that measure the range of interaction in the line theory.

Near the critical point, the gauge theory and necessarily the derived line theory have some operators (for example, the lines themselves) with diverging correlation lengths. However, the range of interaction (as opposed to the correlation length) of the line theory is expected[1] to remain finite at the transition. Reliable analytic approximations to the line theory in the critical region are not available unless N_T is small enough that the transition occurs at large g^2. A numerical approximation is possible if there are correlations that can be measured in the gauge theory which give information on the structure of the line theory.

To find these, begin with finite-temperature, SU(2) lattice gauge theory. The lattice has three spatial directions of infinite extent and one with N_T steps and periodic boundary conditions. The Wilson line at **I**,

$$L(\mathbf{I})=\tfrac{1}{2}\mathrm{Tr}\left[\prod_{I_4} U(\mathbf{I},I_4,4)\right], \tag{2.1}$$

is one-half the trace of the product of the SU(2) matrices on the N_T links in the four-direction at spatial position **I**.

The action for the line theory $s(N_T,g^2,l)$ is defined by integrating all the link variables against the exponential of the gauge theory action and a product of δ functions that fix the lines $L(\mathbf{I})$ to have values $l(\mathbf{I})$:

$$e^{-s}\equiv z\equiv\prod\int dU\, e^{-S}\prod_I \delta(l(I)-L(I)) . \tag{2.2}$$

It follows that

$$Z_s \equiv \prod \int dl\, e^{-s} = \prod \int dU\, e^{-S} \equiv Z_S \tag{2.3}$$

and that

$$\begin{aligned}\langle l(I)\cdots\rangle_s &\equiv \frac{1}{Z_s}\prod \int dl\, e^{-s} l(I)\cdots \\ &= \frac{1}{Z_S}\prod \int dU\, e^{-S} L(I)\cdots \\ &= \langle L(I)\cdots\rangle_S \ .\end{aligned} \tag{2.4}$$

The standard Wilson action

$$S = -\frac{4}{g^2}\sum_P \tfrac{1}{2}\mathrm{Tr}[U(P)] \tag{2.5}$$

will be used.

The line action s is a function of the line configuration. It has parametric dependence on N_T and g^2. The global $Z(2)$ symmetry is

$$s(-l) = s(l) \ . \tag{2.6}$$

A theory with nearest-neighbor couplings includes terms of the form

$$\beta\tfrac{1}{2}\sum_{\text{links}} [l(I)-l(I')]^2 \ . \tag{2.7}$$

The interactions between l's at different sites and their strength can be detected by computing

$$\begin{aligned}-s_{12} &\equiv \frac{\partial^2 s}{\partial l(I_1)\partial l(I_2)} \\ &= \beta \quad \text{if } \mathbf{I}_1 \text{ and } \mathbf{I}_2 \text{ are neighbors} \ .\end{aligned} \tag{2.8}$$

Local potential terms do not contribute when $\mathbf{I}_1 \neq \mathbf{I}_2$.

The line action contains couplings between lines at different sites that are far more complicated than (2.7). The example is very simple in that the interaction between $l(I_1)$ and $l(I_2)$ as measured by s_{12} depends only on the positions I_1 and I_2 and not upon the value of $l(I_1)$ or $l(I_2)$ or any other l. In a general case, $s_{12}(I_1,I_2,l)$ measures the strength of the interaction between $l(I_1)$ and $l(I_2)$, but it may depend upon the configuration of l's in a very complicated manner.

The range of interaction in the line theory is revealed in the behavior of s_{12} as I_1 and I_2 separate. It could be configuration dependent. In some configurations, s_{12} might decay rapidly as the separation increases while in others it might not. The numerical work was done on two kinds of configurations: simple and typical. The simple configurations have all l's equal. The typical configurations have l values taken from gauge theory configurations that were drawn from a distribution generated with e^{-S}. Results for the two cases are surprisingly similar.

It is appropriate to select l values for typical configurations from the gauge field distribution because averages with weight e^{-s} are simply related to averages with e^{-S}:

$$\begin{aligned}-\bar{s}_{12} &= -\frac{1}{Z_s}\prod \int dl\, e^{-s} s_{12}(l) \\ &= -\frac{1}{Z_S}\prod \int dU\, e^{-S} s_{12}(L) \ .\end{aligned} \tag{2.9}$$

Now s_{12} must be expressed in terms of gauge theory correlations that can be approximated analytically or numerically. From (2.2) it follows that

$$-s_1 = -\frac{\partial s}{\partial l(I_1)} = \frac{1}{z} z_1$$

and that

$$-s_{12} = \frac{1}{z} z_{12} - \frac{1}{z} z_1 \frac{1}{z} z_2 \ . \tag{2.10}$$

Subscripts refer to corresponding derivatives as indicated in (2.8).

The derivatives of z can be computed by using the identity

$$\frac{\partial}{\partial l}\delta(l-L) = -\frac{\nabla L}{(\nabla L)^2}\cdot\nabla\delta(l-L) \ . \tag{2.11}$$

The operator in (2.11) is

$$\begin{aligned}\nabla = \nabla(\mathbf{I}) &= \nabla_{A,I_4}(\mathbf{I}) \\ &= (T_A)_{ik} U_{kj}(\mathbf{I},I_4,4)\frac{\partial}{\partial U_{ij}(\mathbf{I},I_4,4)} \ .\end{aligned} \tag{2.12}$$

The T_A are three matrices that generate the fundamental representation of SU(2). Dot products in (2.11) are sums on A and I_4. Invariance of the integration measure implies

$$\int dU\, \nabla f(U) = 0 \ , \tag{2.13}$$

and therefore no surface terms in partial integrations.

Use (2.11) in the expression

$$\begin{aligned}z_1 &= \frac{\partial}{\partial l(I_1)} z \\ &= \prod \int dU\, e^{-S}\delta'[l(I_1)-L(I_1)] \prod_{I\neq I_1} \delta(l-L)\end{aligned} \tag{2.14}$$

and then integrate by parts to obtain

$$z_1 = \prod \int dU\, e^{-S} B(I_1) \prod_I \delta(l-L) \tag{2.15}$$

with

$$B = \nabla\cdot\frac{\nabla L}{(\nabla L)^2} - \frac{\nabla L}{(\nabla L)^2}\cdot\nabla S \ . \tag{2.16}$$

Thus

$$\begin{aligned}-s_1 = \frac{1}{z} z_1 &= \frac{\prod \int dU\, e^{-S} B(I_1) \prod \delta}{\prod \int dU\, e^{-S} \prod \delta} \\ &\equiv \langle B(I_1)\rangle_z \ .\end{aligned} \tag{2.17}$$

A similar calculation gives

$$z_{12}=\prod\int dU\, e^{-S}[B(I_1)B(I_2)-C(I_1,I_2)]\prod\delta \tag{2.18}$$

with

$$C(I_1,I_2)=-\frac{\nabla L_2}{(\nabla L_2)^2}\cdot\nabla_2 B(I_1)\ . \tag{2.19}$$

Thus

$$\frac{1}{z}z_{12}=\langle B(I_1)B(I_2)-C(I_1,I_2)\rangle_z \tag{2.20}$$

and

$$-s_{12}=\langle B(I_1)B(I_2)\rangle_z^C-\langle C(I_1,I_2)\rangle_z\ . \tag{2.21}$$

The first term on the right-hand side of (2.21) is the connected correlation function.

Since the configuration of the L's is fixed by δ functions, the first term in (2.16) is a constant that does not contribute to the connected correlation in (2.21). B can be replaced by

$$B_0=-\frac{\nabla L}{(\nabla L)^2}\cdot\nabla S \tag{2.22}$$

in (2.21) and also in (2.19) if $I_1\neq I_2$. C is zero unless I_1 and I_2 coincide or are nearest neighbors.

It is straightforward to work out the derivatives in B_0 and C:

$$B_0(\mathbf{I})=-\frac{4}{g^2}\frac{1}{1-l(\mathbf{I})^2}\frac{1}{N_T}\sum_{I_4}\sum_{\mu=\pm1,\pm2,\pm3}[b_1(\mathbf{I},I_4,\mu)-b_2(\mathbf{I},I_4,\mu)]\ , \tag{2.23}$$

$$C(\mathbf{I},\mathbf{I}+\hat{\mu})=-\frac{4}{g^2}\frac{1}{N_T^2}\frac{1}{1-l(I)^2}\frac{1}{1-l(I+\mu)^2}\sum_{I_4}[c_1(\mathbf{I},I_4,\mu)-c_2(\mathbf{I},I_4,\mu)-c_3(\mathbf{I},I_4,\mu)+c_4(\mathbf{I},I_4,\mu)]\ . \tag{2.24}$$

The b's and c's are best expressed in pictures. Please refer to Figs. 1 and 2. Paths in the four-direction are closed by the periodic boundary conditions. Closed paths in the figures are to be understood as one-half the trace of the product of the indicated link matrices. When there are multiple closed paths the half traces are to be multiplied together.

Now it is evident that the expression for $\bar{s}_{12}$ in (2.9) is a bit more involved than it appears. The evaluation of s_{12} for each configuration is an average of the type $\langle\ \rangle_z$.

The evaluation of these averages can be simplified a little by the following observation. An arbitrary gauge field configuration includes a specification of the group elements on the four-direction links. These yield values for the lines L. Consider another set of four-direction matrices that gives the same values for the lines. It is not difficult to show that the first configuration is gauge equivalent to one with the second set of four-direction matrices. Thus the $\langle\ \rangle_z$ averages may be computed by fixing the four-direction matrices to values that give the desired L's and then integrating over the spatial link matrices only.

The quantity s_{12} is a suitable measure of the range of interaction in the line theory. It has been expressed in a form that can be used in a Monte Carlo simulation.

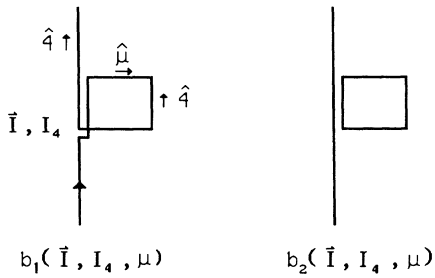

FIG. 1. The products of links for Eq. (2.23).

III. NUMERICAL EXPERIMENT

This section describes a numerical approximation of s_{12}. The results indicate that the range of interaction is very short.

s_{12} depends upon the configuration of lines, N_T, and g^2. For each value of these arguments, it is an average $\langle\ \rangle_z$. As indicated in (2.17), these averages are computed as conventional integrations over spatial links with four-direction links fixed to give the desired L's. The integrations over the group elements on spatial links are done

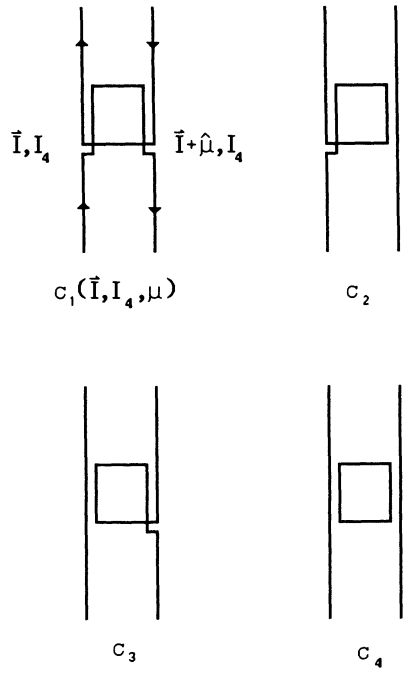

FIG. 2. The products of links for Eq. (2.24).

with a conventional heat-bath Monte Carlo simulation. The techniques are similar to those described in Ref. 3.

s_{12} was computed for nine configurations of lines. Since the universality arguments apply to the critical region, it is most interesting to look at s_{12} in this region. At the value $N_T=4$ that is used, the critical coupling $4/g_c^2$ is about 2.296 (Ref. 2). Earlier work[3] indicates that the couplings 2.275 and 2.285 are within the critical region and have associated line-line correlation lengths of 4.5 and 6.25, respectively. From configurations produced in that work, seven were selected. Configurations 1, 2, and 3 were taken from the sample at $4/g^2=2.275$ and $N_S^3\times N_T=11^3\times 4$. They are at iterations 5000, 7000, and 9000. Number 4 is iteration 4000 in a sample at 2.275 and $15^3\times 4$. Numbers 5, 6, and 7 are iterations 10 000, 15 000, and 22 000 from the collection at 2.285 and $15^3\times 4$. These configurations were not inspected or screened for any characteristics before selection. In the eighth starting configuration, all spatial links on a $15^3\times 4$ lattice are equal to 1 and all four-direction links are equal to $\exp(i\sigma_3\pi/8)$. This gives $L(\mathbf{I})=0$. The ninth is similarly arranged to give $L=0.1$. The last two are useful as reference examples.

Monte Carlo runs began with these nine configurations and updated the spatial links without altering the four-direction links. For cases 1–4, $4/g^2=2.275$, and for 5–9, 2.285. Cases 1–7 received 5000 sweeps each while cases 8 and 9 got 3000 each. After each sweep, data for a calculation of s_{12} were computed and saved. The measured quantities stabilized rapidly, and just 200 sweeps were dropped for equilibration.

Since the first seven configurations of lines are not homogeneous, s_{12} will depend separately on $\mathbf{I}_1$ and $\mathbf{I}_2$. Impractically long runs would be needed to beat down the fluctuations on these quantities. The spatial averages

$$s''(\mathbf{J})=\frac{1}{N_S^3}\sum_{\mathbf{I}} s_{12}(\mathbf{I},\mathbf{I}+\mathbf{J}) \tag{3.1}$$

which are more easily measured will be reported.

Results are presented in the figures. Figure 3 is a semilogarithmic plot of s'' for cases 1–4. The plotted values are an average of all the data from J's with the same lattice distance $|\mathbf{J}|$. On the horizontal axes of the figures, $J=|\mathbf{J}|$. Figure 4 is an average of the same data compared with the scalar lattice propagator:

$$D(I,Z,\xi)=\frac{1}{N_S^3}\sum_K e^{iK\cdot I}\frac{Z}{\sum_\mu (1-\cos K_\mu)+\xi^{-2}}\ . \tag{3.2}$$

This function is convenient for purposes of comparison because it has a roughly exponential decay with scale ξ and correctly includes finite-size and finite-spacing lattice effects. The two cases that are used for illustration are $\xi=1.0$ and 0.5 with arbitrary normalization Z. (The irregular behavior of D is a lattice effect that arises when ξ is small. It is associated with the lack of rotational invariance for small ξ and I.) Figures 5 and 6 display data from cases 5–7 while Figs. 7 and 8 present cases 8 and 9.

There are several notable features of these results. In all cases, s'' falls rapidly with separation. The rate is comparable to $D(I,\xi=0.5)$ and certainly faster than $D(I,\xi=1.0)$. This indicates that the range of interaction is short.

Cases 1–4 behave similarly as do cases 5–7. Although the samples are small, this indicates that the results are probably representative of a larger sample and therefore

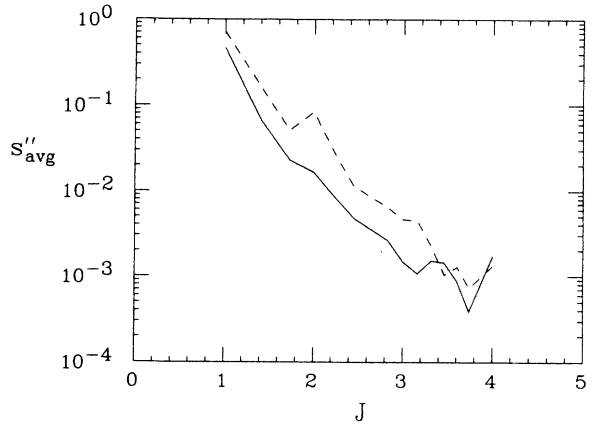

FIG. 4. The average of cases 1–4 (solid line) compared with $D(J,\xi=0.5)$ (dashed line) and $D(J,\xi=1.0)$ (dotted line).

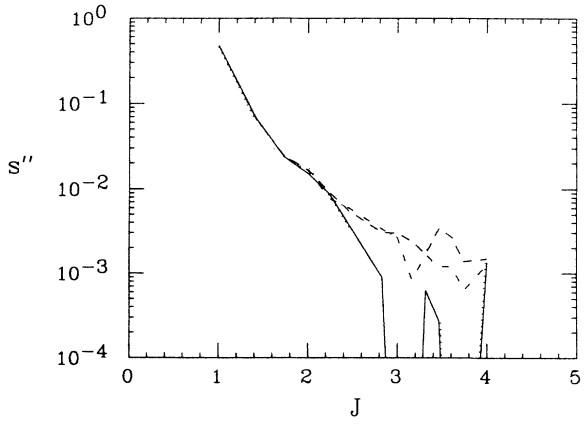

FIG. 3. $s''(J)$ for cases 1–4. $4/g^2=2.275$.

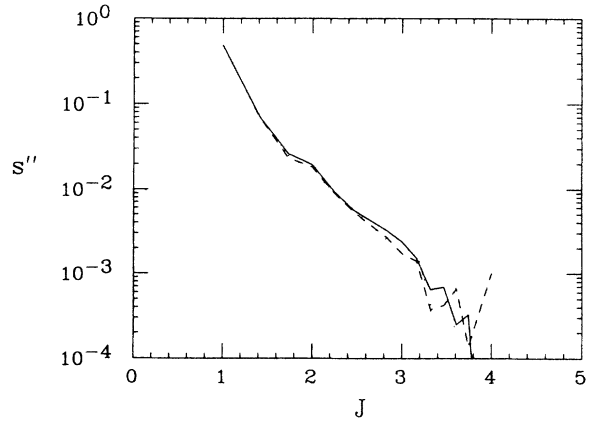

FIG. 5. $s''(J)$ for cases 5–7. $4/g^2=2.285$.

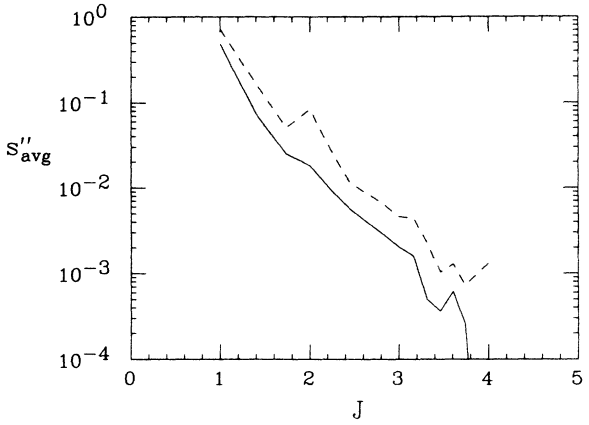

FIG. 6. The average of cases 5–7 (solid line) compared with $D(J,\xi=0.5)$ (dashed line) and $D(J,\xi=1.0)$ (dotted line).

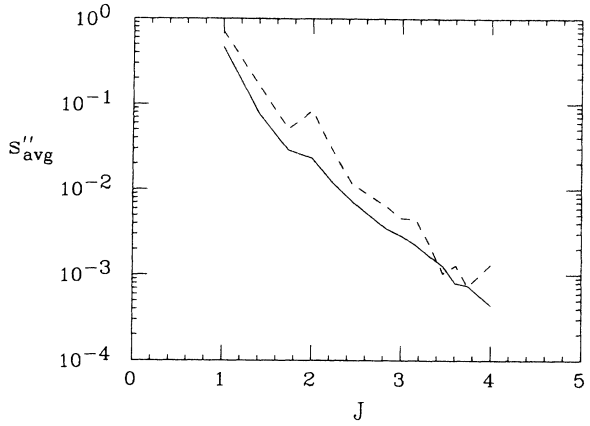

FIG. 8. The average of cases 8 and 9 (solid line) compared with $D(J,\xi=0.5)$ (dashed line) and $D(J,\xi=1.0)$ (dotted line).

of the physics in this region.

The $4/g^2=2.285$ cases do not noticeably differ from those at $4/g^2=2.275$. This indicates that the nature of the line-line interaction is not changing rapidly as the critical point is approached.

Surprisingly, the constant L data for cases 8 and 9 do not differ much from that for the typical L cases. The typical L cases are in the confined phase and thus from an ensemble with $\langle L\rangle=0$. The values for $\langle L\rangle$ and $(L-\langle L\rangle)_{\rm rms}$ in Table I show that L's are very nearly uniformally distributed relative to the weight $(1-L^2)^{1/2}$ that is passed along from the SU(2) group measure. The constant L cases have $L=0$ or $L=0.1$ and no variation over the lattice. So while the typical and constant cases have similar $\langle L\rangle$'s, they are very different configurations. Nevertheless the range of interaction of the lines is about the same for the two kinds of configurations.

It is possible that $s_{12}(I,I+J)$ could be large and positive at some I's, large and negative at others, with cancellations in (3.1) leading to a misleadingly small value for $s''(J)$. The configurations with constant L shed some light on this issue. In these cases, s_{12} depends on the separation so that there will not be cancellations in the sum in (3.1). Again there is a rapid decay with separation. Also s_{12} is even in $L\rightarrow -L$. These two facts indicate that if there are cancellations in (3.1) that allow slow decays of $s_{12}(I,I+J)$ but give rapid decays for $s''(J)$, then it would have to be arranged in a fairly tricky manner. Although this possibility has not been excluded, it seems unlikely and there is nothing to support it at this point.

It is also possible that in addition to the rapidly decaying interaction that is observed, there could also be a weak long-range interaction that is hidden in the noise.

Since the data have been given without error bars a brief remark is in order. The quantity of interest is not the value of $s''(J)$ but rather the rate of decay with increasing J. Point-by-point error bars could be given. However, on a given line, they are highly correlated and greatly overestimate the uncertainty in the decay rate. The technique[3] of splitting a run of 5000 sweeps into 5 runs of 1000 sweeps and measuring the decay of s'' on each of these would be more meaningful. However, it is just as enlightening to observe that the different cases are uncorrelated so that the uncertainty in the decay rate for each case is no larger than the amount by which the cases differ in decay rate.

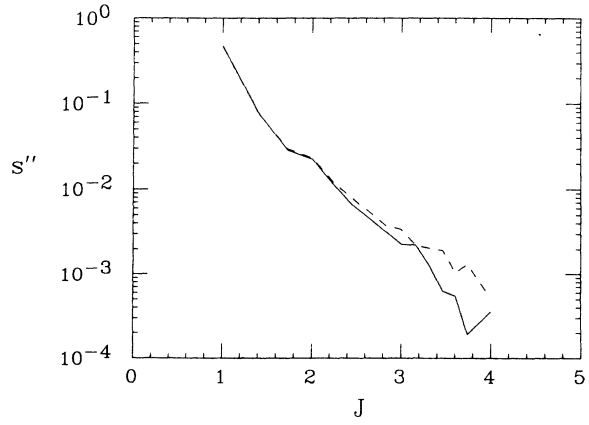

FIG. 7. s'' for cases 8 (solid line) and 9 (dashed line). $4/g^2=2.285$.

TABLE I. Values of $\langle L\rangle$ and $(L-\langle L\rangle)_{\rm rms}$ for the nine line configurations.

	$\langle L\rangle$	$(L-\langle L\rangle)_{\rm rms}$
1	0.0431	0.4967
2	−0.0726	0.4911
3	0.1332	0.4832
4	−0.0791	0.4970
5	−0.0139	0.4938
6	−0.0064	0.5108
7	0.0428	0.4969
8	0.0000	0.0000
9	0.1000	0.0000

IV. CONCLUSION

Section II gave the theoretical basis for the numerical work. It introduced the quantity s_{12} which gives a measure of the range of interaction in the effective line theory. The numerical results in Sec. III provide strong support for the claim that the effective line theory has short-range interactions. The range is less than one when the correlation length is 6.25. Further studies of the structure of the effective line theory can build on this basic property.

ACKNOWLEDGMENTS

General support for this research was provided by the Department of Energy. The numerical work was done on the DOE-supported CRAY's at the National Magnetic Fusion Energy Computer Center and on the NSF-supported CRAY at the San Diego Supercomputer Center. I would like to thank M. Golterman and K. Sparks for reading the manuscript.

[1]B. Svetitsky and L. Yaffe, Nucl. Phys. **B210** [FS6], 423 (1982); J. Kuti, J. Polonyi, and K. Szlachanyi, Phys. Lett. **110B**, 395 (1982); F. Green and K. Karsch, Nucl. Phys. **B238**, 297 (1984); M. Ogilvie, Phys. Rev. Lett. **52**, 1369 (1984); N. Weiss, Phys. Rev. D **24**, 475 (1981); **25**, 2667 (1982); M. Gross, Phys. Lett. **132B**, 125 (1983); T. Banks and A. Ukawa, Nucl. Phys. **B225** [FS9], 145 (1983).

[2]L. McLerran and B. Svetitsky, Phys. Lett. **98B**, 195 (1981); J. Kuti, J. Polonyi, and K. Szlachanyi, *ibid.* **98B**, 199 (1981); L. McLerran and B. Svetitsky, Phys. Rev. D **24**, 450 (1981); R. Gavai and H. Satz, Phys. Lett. **145B**, 248 (1984); C. Curci and R. Tripiccione, *ibid.* **151B**, 145 (1985); J. Engels, F. Karsch, I. Montvay, and H. Satz, Nucl. Phys. **B205** [FS5], 545 (1982); S. Das and J. Kogut, *ibid.* **B265** [FS15], 303 (1986); Phys. Lett. B **179**, 130 (1986); J. Kogut, M. Stone, H. Wyld, W. Gibbs, J. Shigemitsu, S. Shenker, and D. Sinclair, Phys. Rev. Lett. **50**, 393 (1983); M. Gross and J. Wheater, Nucl. Phys. **B240** [FS2], 253 (1984); K. Kanaya, Report No. BI TP 85/21 (unpublished); K. Kanaya and H. Satz, Phys. Rev. D **34**, 3193 (1986); J. Engles, J. Jersak, K. Kanaya, E. Laermann, C. Lang, T. Neuhaus, and H. Satz, Nucl. Phys. **B280**, 577 (1987); P. Suranyi and P. Harten, Phys. Rev. D **35**, 1979 (1987).

[3]J. Kiskis, Phys. Rev. D **33**, 2380 (1986); **35**, 1456 (1987).

[4]A. Gonzales-Arroyo and M. Okawa, Phys. Rev. Lett. **58**, 2165 (1987); J. Deckert, S. Wansleben, and J. Zabolitzky, Phys. Rev. D **35**, 683 (1987).